Study of a trailing shield for electrical arc manufacturing processes – 3D multi-physical modelling of gas flow and prediction of shielding efficiency

S. Morville[1], A. Benoît[1]
1. IRT Jules Verne, Bouguenais, France

Introduction

Arc welding and arc additive manufacturing processes involve an electrical arc plasma used as a high-density heat source for melting and joining/growing of metal parts, with an inert gas for plasma ignition and shielding of hot areas. Indeed, metal may be highly sensitive to oxygen content. Consequently, design of a suitable and robust shield becomes a relevant issue. The scope of this paper is providing a numerical methodology in order to deepen the understanding of phenomena involved in gas flow, highlighting some relationships between design, process parameters and surfaces protection. A three-dimensional CFD model is implemented in Comsol Multiphysics® with a RANS turbulence model. Additionally, a transport equation of highly concentrated species is included, dealing with couplings with gas flow, i.e. turbulent diffusion and Buoyancy. Results show effects of the design on the gas flow and shielding efficiency.

Keywords: trailing shield, 3D modelling, turbulent gas flow, mass transport, oxygen content, shielding efficiency, WAAM

Background

Oxygen is a chemical element that reacts with metals heated to high temperatures. In order to prevent the resulting oxidation phenomena, a local inert gas shield is commonly used. Purpose of this active flow is for stopping the migration of oxygen present in the air. Otherwise, that may lead to the creation of an oxides layer and a lower wettability of the melt pool, a drop of mechanical properties and oxidization of solid surfaces beyond a few hundred degrees Celsius. For industrial welding applications, it is common to use a trailing shield which blows a pure argon flow. The design of the trailing shield plays a critical role in the efficiency of the device, namely its ability to control the flow in such a way as to prevent any entry of oxygen toward hot areas. However, most of trailing shields are restricted to specific applications and shielding efficiency is strongly dependent on know-how of welders. Basically, trailing shield are boxes supplied with inert gas. The underside is designed with a device for diffusing a homogeneous and smooth gas flow.

Several publications from literature report numerical studies related to welding arc shield [1-4] and fume extraction [5]. In most cases, the study is located on the melt pool. These approaches deal very comprehensively with the physics of arc plasma and focus on the characteristics of the flow around the welding gun. However, the evolution of the gas shield after metal solidification is not studied, while oxygen comes back in contact with the hot surfaces. However, Jäckel et al. proposed a relevant approach dealing with the whole shielding gas flow from both welding gun and trailing shield [6], where authors demonstrated the capability of a multi-physic CFD model for predicting shielding efficiency in a practical use case.

In a same way as [6], this work focuses on the study of the trailing shield used to protect the deposited material. To this end, the design of the material shown in Figure 1 was used for generating a CAD. Pictures show the fixture, the gas supply through the blue pipe, the side barriers used for confining the flow, and the diffuser. This one consists of a perforated metal plate and a double layer of wire gauze ensuring the smoothing of the gas flow. The objective is the implementation of a multiphysics model able to describe the flows of this trailing shield and its shielding efficiency within the scope of a welding operation, which is the targeted application, then of an additive manufacturing operation.

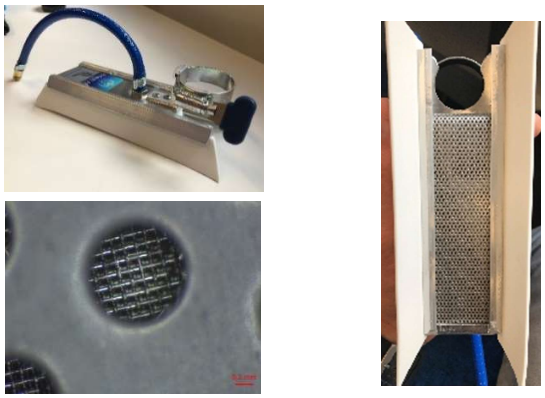

Figure 1. TITECH PRO™ trailing shield used for standard welding applications

Numerical model

The following sections provide information on the physical model and assumptions, main governing equations, initial and boundaries conditions, discretization and solver.

Physical assumptions

The set of governing equations assumes a low-compressible flow (Ma<0.3). CFD module is used here and involved Reynolds-Averaged Navier-Stokes equations with a Shear-Stress Transport turbulence model for describing unsolved sub-scales of the gas flow. A transport conservative equation is included, dealing with mixture of welding gas and air (a Fick's law describes diffusion flux). Chemical composition of air is fixed (21% O_2 – 79% N_2) and demixing effects induced by electrical fields, pressure gradients and thermal gradients are neglected here. Consequently, two species are described by the

transport equation: air and argon. While the impact of molar fraction on molecular diffusion is neglected, the local molecular weight assumes a mixture with a variable density given by the perfect gas law. Therefore, Buoyancy phenomenon induced by chemical content changes is taken into account by the simulation. Extra-diffusion induced by eddies are considered through the turbulent kinematic viscosity given by the RANS model. Finally, dynamic viscosity of argon is close to air as well, and then they are assumed to be the same.

In this work, some strong modelling assumptions are made. (1) The electrical arc plasma is neglected and studies are focused on the trailing shield flows only. However, a simplified design of the welding gun is included, dealing with gas flow used for plasma ignition and melt pool shielding. (2) The existence of a turbulent steady-state gas flow is allowed. (3) Gas flow exhibits a plane of symmetry in the longitudinal direction.

Governing equations

Simulations are performed with Comsol Multiphysics 5.5, plus CFD module. Main solved equations are the following:

Reynolds-Averaged Navier-Stokes equations

$$\rho(\mathbf{u}\cdot\nabla)\mathbf{u} = \nabla(-p\mathbf{I}+\mathbf{K}) + \rho\mathbf{g} \quad (1)$$

$$\mathbf{K} = (\mu_i+\mu_T)(\nabla\mathbf{u}+(\nabla\mathbf{u})^T) - \frac{2}{3}(\mu+\mu_T)(\nabla\cdot\mathbf{u})I - \frac{2}{3}\rho k\mathbf{I} \quad (2)$$

$$\nabla\cdot(\rho\mathbf{u}) = 0 \quad (3)$$

Perfect gas law equation

$$\rho = \frac{p_{ref}M_{mix}}{RT}\ ;\ M_{mix} = \left(\sum_{i=1}^{j}\frac{x_i}{M_i}\right)^{-1} \quad (4)$$

Mass transport equation

$$\nabla\cdot\left((D_i+D_T)\nabla c_i\right) + \mathbf{u}\cdot\nabla c_i = 0 \quad (5)$$

where ρ is the gas density addressed by the perfect gas law ($kg.m^{-3}$), **u** is the velocity vector ($m.s^{-1}$), p is pressure (Pa), **I** is identity matrix, **g** is gravity vector, μ and μ_T are standard and turbulent dynamic viscosities respectively (Pa.s), k is turbulent kinematic energy ($m^2.s^2$), p_{ref} is atmospheric pressure (Pa), x_i and M_i are the molar fraction and molecular weight ($kg.mol^{-1}$) of the chemical specie i, D_i and D_T are coefficients of molecular and turbulent diffusion ($m^2.s^{-1}$), c_i is the molar concentration ($mol.m^{-3}$).
Equations related to the SST turbulent model are not reported here, but available in the CFD module documentation [7].

Parameters and material properties used in simulations are given in the following table:

Table 1: Selected parameters and gas properties

Reference temperature, T_{ref}	293 K
Reference pressure, p_{ref}	1 atm
Molecular weight of air, M_{air}	0.029 $kg.mol^{-1}$
Molecular weight or argon, M_{Ar}	0.04 $kg.mol^{-1}$
Dynamic viscosity, μ_i	$2x10^{-5}$ Pa.s
Diffusion coefficient, D_i	0.148 $cm^2.s^{-1}$
Welding gun gas flow, Q_g	15 $L.min^{-1}$
Trailing shield gas flow, Q_s	10 $L.min^{-1}$
Welding velocity, V_d	30 $cm.min^{-1}$

Initial conditions and boundaries conditions

Regarding the description of the physical model, constant temperature and pressure are assumed at 293K and 1 atmosphere respectively, and initial molar fraction is 100% air. Inlet gas flows are defined with 100% argon gas flow rates. External surfaces are open boundaries with a normal flow constraint, which improves the robustness of convergence during solver iterations. Inward flows assume a fixed molar fraction equal to air value, while outward flows ignore diffusive transport. A uniform slip velocity is applied on the workpiece flat surface and simulates the relative displacement between the fixed workpiece and the moving gun torch.
A particular attention is paid to the description of the wire gauze used for smoothing the gas flow. A fine modelling of gas flow through the grid is unthinkable regarding issues for the grid mesh generation and a high scale factor of the wire gauze. Then effects of wire gauze are taken into account by a screen interior boundaries where correlations for resistance and refraction coefficients are included. Parameters of correlations are based on solidity of the metal mesh and wire diameter (please refer to the CFD module documentation for details about theory and equations of screen modelling). Such analytic model is highly sensitive to transversal flows, that is the reason why screen surfaces are located at mid-thickness of the drilled holes. Similar approach is not workable for the perforated plate once it assumes a screen with equivalent properties, i.e. cross-section of holes is spread over the whole plate. Consequently, effects on flow distribution would have been underestimated.

Discretization and solvers

Resolution of any 3D turbulent CFD simulations is a numerical challenge and a suitable balance between computational time and accuracy of the solution is needed. Geometry is locally refined inside the trailing shield due to high velocities gradients and complex flows (0.25-1mm, see **Figure 2**). Areas of interest (below the trailing shield and at the fringes) are also refined (1mm), while the grid mesh is a bit coarser away (5mm). Finally, a 4-elements boundary layer mesh is automatically generated on solid surfaces. Total number of elements are 939,744 for the internal domain and 1,699,100 for the external domain.

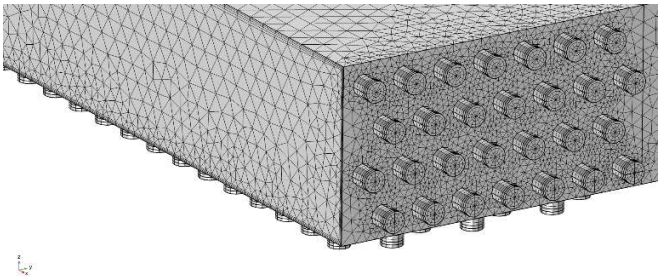

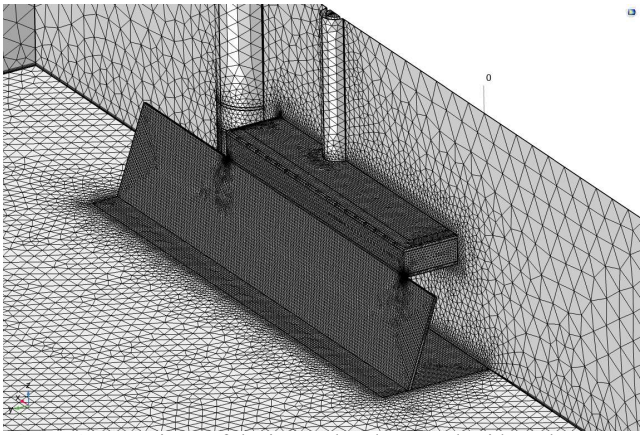

Figure 2. Overviews of the internal and external grid mesh generated with Comsol Multiphysics

A standard study is divided into two steps: first one is an initialization to the wall distance and second one a stationary resolution. Due to high computation costs and significant non-linearities induced by those simulations, a segregated solver is used for step 2, where chemical transport and Navier-Stokes equations are at the first step while turbulence equations are merged in another one. Default iterative solvers and suggested settings give good convergence rate and were unchanged. Computational time is about 12h for solving 4,091,821 degrees of freedom with a 12 cores - 192 Go RAM workstation.

Simulation Results

Welding application

Hereafter, all color scales of the velocities norm are upper limited at 1 $m.s^{-1}$, that minimizes the effect of maximal values on color range. **Figure 3** gives an overview of the gas flows inside the trailing shield. Inlet pipe orientation makes argon splashing onto the perforated plate and rotating inside the cavity. Then outward flowrates are highly impacted by the balance between dynamic pressure induced by high velocities, external pressure, and pressure losses from the perforated plate and wire gauze. For information, internal overpressure is 55 Pa and averaged outlet velocity is 0.28 $m.s^{-1}$ with a 10 $L.min^{-1}$ gas flowrate.

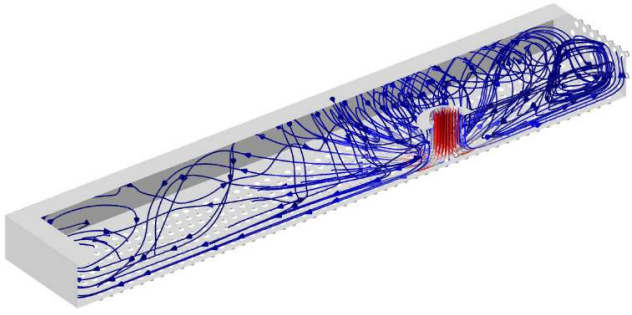

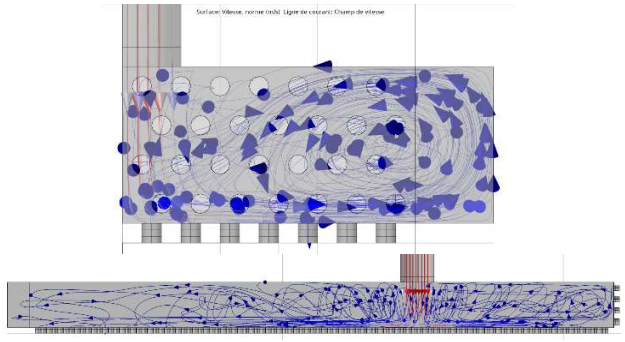

Figure 3. Different views of the steady-state flow (perspective, front, side)

Figure 4 focuses on outlets of the perforated plate. The bottom view highlights three areas. The first one is located in front of the argon inlet pipe, where flow is perpendicular to the surface and outward velocity is higher than 1 $m.s^{-1}$. The second one is peripheral to the first one. Surface parallel flow leads to inward and outward velocities with low magnitudes (> 0.1 $m.s^{-1}$). Consequently, few volumes of external gas are captured due to negative relative pressure. That may lead to an oxygen pollution of the blown gas. The third area shows a homogeneous field of outward velocities (0.4 $m.s^{-1}$). Front view of the outlets shows similar trends, namely outlet holes with high flow speed (< 1 $m.s^{-1}$) due to the coming surface parallel flow showed in the right side of **Figure 3**.

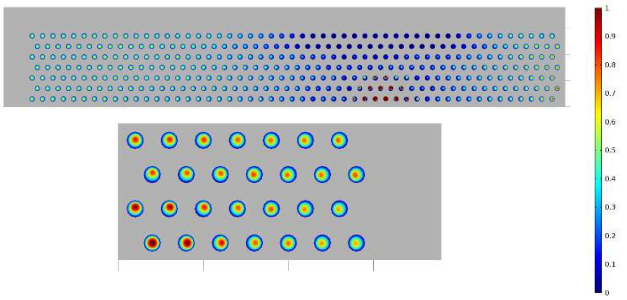

Figure 4. Bottom view and front view of the trailing shield outlets (magnitude of velocities norm)

Different designs were investigated for an improvement of the distribution of flow rates (not discussed in this paper): closing holes, spray deflector, two perforated plates and alternative diffuser.

The numerical solution of the external flow is illustrated in **Figure 5**, including both trailing shield and welding gun. Lateral barrier maintains the argon flow in the tunnel, which generates many vortices. The tunnel effect induced by the barrier constraints the gas flow moving outside and welding gas being heavier than air, Buoyancy makes argon to naturally fall also, as a creeping flow. Consequently, convective transport counters diffusive fluxes driven by gradients of partial pressure. Estimated O_2 content is very low (<100 ppm, see the gray isosurface in **Figure 5**), which confirms the efficiency of this design for welding application.

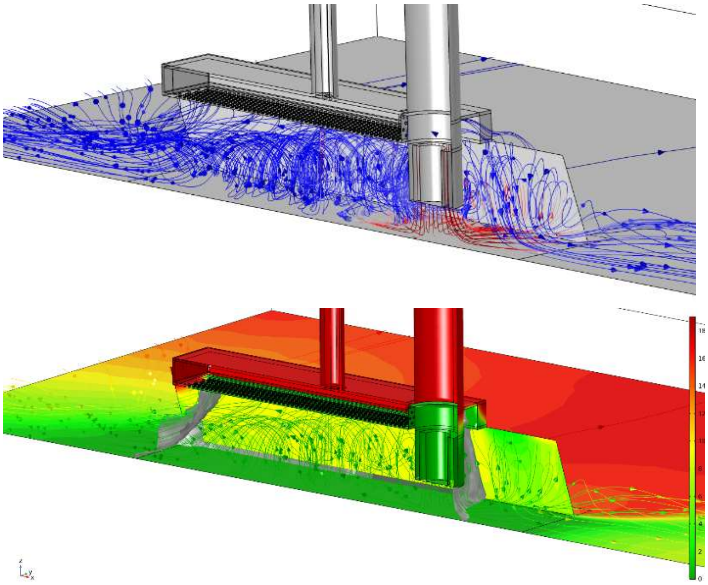

Figure 5. External flows induced by welding gun and trailing shield flowrates (top picture: colored streamlines based on velocities norm; bottom picture: colored streamlines based on O_2 content)

Discussion

First simulations give encouraging results regarding the capability to assess the shielding efficiency with the present modelling. Next step focuses on another configuration related to additive manufacturing with gap between the trailing shield and the workpiece, and different flowrates.

Additive manufacturing application

The metal additive manufacturing application is simulated by printing a straight wall of 5 mm height (**Figure 6**). Distance between the welding gun and the melt pool being maintained, the trailing shield is therefore raised by the same height. In fact, a gap appears between the flat surface and the side barrier. Though small, this space is sufficient to break the confinement of the argon and the flow spreads directly onto the flat surface. Air is then observed to enter from front and rear of the trailing shield. That results in the oxygen contamination of the surfaces. This pollution is highlighted at the position of the 100 ppm oxygen isovalue, much less extensive than in the case of the welding application.

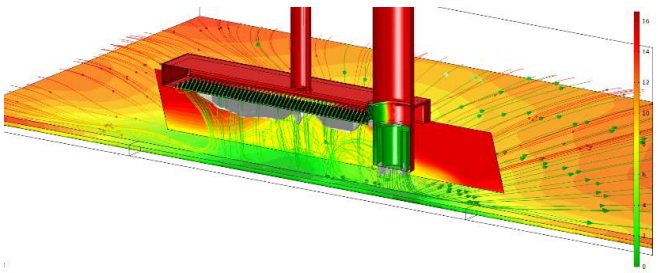

Figure 6. External flows during printing of a 5mm height wall (colored streamlines based on O_2 content)

Additional calculations were carried out with gas flow rates multiplied by a factor of 2 to 10, which improved the extent of the gas shield. However, gas flow rates involved become very high and the economic cost induced does not make this solution viable. Finally, calculations made with an extended height of wall (80 mm) have shown the difficulty in shielding the wall (**Figure 7**), whatever the flow rate (**Figure 8**).

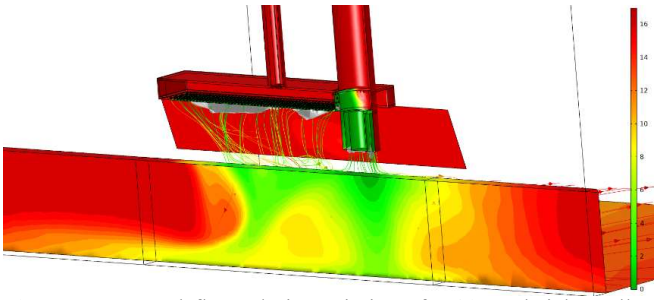

Figure 7. External flows during printing of a 80mm height wall at nominal flow rate (colored streamlines based on O_2 content)

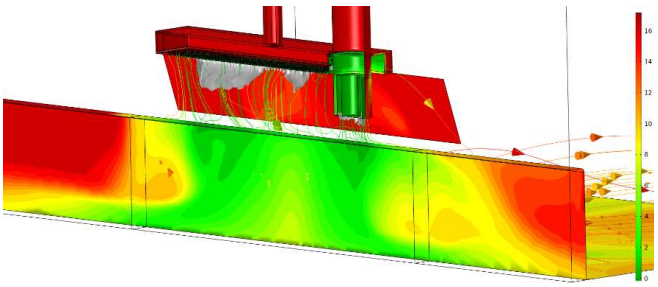

Figure 8. External flows during printing of a 80mm height wall with 10 time the nominal flow rate (colored streamlines based on O_2 content)

Conclusions

This paper deals with a shielding gas issue on electric arc applications, and a multiphysics model has been implemented for describing this phenomenon. The Navier-Stokes equations are coupled with an SST turbulence model and a mass transport equation. This set of equations allows for predicting the oxygen content in the gas phase based on process parameters and the geometry of a trailing shield. The internal flows are finely described in order to predict the distribution of the gas flow by considering the different kinds of pressure losses. Behavior of the trailing shield is described in the case of a welding application, and the results obtained are satisfactory since the simulation finds a suitable shielding efficiency for a nominal configuration. The trailing shield has been extrapolated to an additive manufacturing application. Results tend to show a drop of the shielding efficiency as soon as there is no longer contact between the trailing shield and the workpiece, and increasing flow rates is not a viable adjustment variable from an economic point of view.

Reliability of this model could be improved subsequently by integrating various evolutions: taking into account effects of the arc plasma which induce thermal Buoyancy and Lorentz forces, taking into account the heat transfer trough the part which is evolutionary during additive manufacturing, dealing with unsteady state and a full 3D description of the flows.

References

1. M. Schnick, M. Dreher, J. Zschetzsche, U. Fuessel, A. Spille-Kohoff, “Visualisation and optimization of shielding gas flows in arc welding”, Welding in the world, **Vol. 56**, 54-61 (2012)
2. M. Hässler, S. Rose, U. Füssel, “The influence of arc interactions and a central filler wire on shielding gas flow in tandem GMAW”, Welding in the world, **Vol. 60**, 713-718 (2016)
3. I. Bitharas, N.A. McPherson, W. McGhie, D. Roy, A.J. Moore, “Visualisation and optimization of shielding gas coverage during the GMAW”, Journal of Materials Processing Tech., **255**, 451-462 (2018)
4. M. Schnick, G. Wilhelm, M. Lohse, U. Füssel, A.B. Murphy, “Three-dimensional modelling of arc behavior and gas shield qyality in tandem gas metal arc welding using anti-phase pulse synchronization”, Journal of Physics D: Applied Physics, **44**, 185-205 (2011)
5. P. Cooper, A.R. Godbole, J. Norrish, “Modelling and simulation of gas flow in arc welding – Implications for shielding efficiency and fume extraction”, Revista Soldagem and Inspecao, 12 (4), 336-345 (2007)
6. S. Jäckel, M. Hertel, U. Füssel, “Design of a gas trailing shields for TIG-welding of stainless steels”, Welding in the World, **61**, 117-123 (2017)
7. Comsol Multiphysics, CFD module user’s guide, link